



# Pulling the Levers of Photophysics: How Structure Controls the Rate of Energy Dissipation\*\*

Thomas S. Kuhlman, Michael Pittelkow, Theis I. Sølling,\* and Klaus B. Møller\*

The process of internal conversion is at the heart of many chemical reactions by being responsible for the conversion of electronic excitation energy into vibrational energy.<sup>[1,2]</sup> The ultrafast process from higher electronic states assures that it can rival competing pathways. This also implies that nuclear motion in only a very few vibrational degrees of freedom are involved in internal conversion—if more were to take part the rate of energy dissipation would simply not be able to compete with the rate of photochemical reaction or radiative transition. This is inherently different from thermalized reactions where the total number of degrees of freedom of the system influences the rate of reaction because of the statistical distribution of energy. Such statistical behavior is not necessarily observed by ultrafast, excited-state reactions.<sup>[3–5]</sup>

A general picture of the structural parameters that control the rate of an internal conversion process leading to energy dissipation is not easily deducible. Herein, we demonstrate how the rate of such an internal conversion process can change by more than an order of magnitude for related molecules as a consequence of minor structural variations. We disentangle the complex process and identify one specific vibrational mode involved through the use of the techniques time-resolved mass-spectrometry (TRMS) and time-resolved photoelectron spectroscopy (TRPES) on four molecules: 2-methylcyclobutanone (2-MeCB), 2-methylcyclopentanone (2-MeCP), 3-methylcyclopentanone (3-MeCP), and 3-ethylcyclopentanone (3-EtCP). These four molecules are structurally similar to cyclobutanone (CB), cyclopentanone (CP), and cyclohexanone (CH) investigated in our previous works (Figure 1).<sup>[6,7]</sup>

Following excitation to  $S_2$ , ( $n,3s$ ) state, the temporal evolution of the ion currents presented in Figure 2 closely resemble that of the ( $n,3s$ ) photoelectron peak also given in the figure for 2-MeCB and 2-MeCP. Consequently, the decay

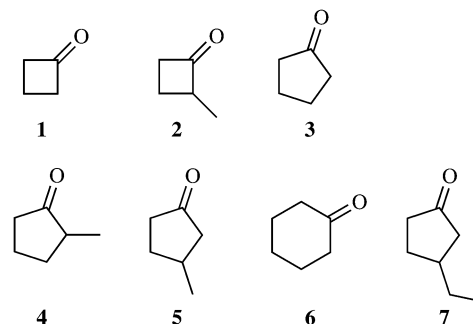


**Figure 1.** Molecules considered in this study with the number of internal degrees of freedom given in parentheses. 1: cyclobutanone (27), 2: 2-methylcyclobutanone (36), 3: cyclopentanone (36), 4: 2-methylcyclopentanone (45), 5: 3-methylcyclopentanone (45), 6: cyclohexanone (45), and 7: 3-ethylcyclopentanone (57).

in the ion yield can be used as a measure of the lifetime of the ( $n,3s$ ) state. A similar relationship was observed for the unsubstituted cycloketones.<sup>[6]</sup> The ion currents reveal a set of timescales for the ( $n,3s$ )→( $n,\pi^*$ ) transition, that is,  $S_2$ → $S_1$ , and thereby for the conversion of part of the electronic energy of the system into vibrational energy, ranging over more than an order of magnitude from  $0.37 \pm 0.01$  ps for 2-MeCB to  $5.79 \pm 0.16$  ps for 3-MeCP (Table 1). A clear grouping of the timescales is seen in terms of the ring size. For a particular

**Table 1:** Timescales for the decay of the parent ion current for the substituted cycloketones along with their unsubstituted species after excitation to the ( $n,3s$ ) state.

Molecule	$\tau_1$ [ps]	$\tau_2$ [ps]
cyclobutanone <sup>[a]</sup>	$0.08 \pm 0.01$	$0.74 \pm 0.01$
2-methylcyclobutanone	$0.08 \pm 0.01$	$0.37 \pm 0.01$
cyclopentanone <sup>[a]</sup>		$5.39 \pm 0.17$
2-methylcyclopentanone		$3.05 \pm 0.01$
3-methylcyclopentanone		$5.79 \pm 0.16$
3-ethylcyclopentanone		$5.16 \pm 0.17$
cyclohexanone <sup>[a]</sup>		$9.67 \pm 0.43$

[a] From Ref. [6].

ring size substitution in the 2-position but not in the 3-position leads to a faster transition. Here we disentangle the dynamical process to identify specific properties leading to these inter- and intragroup timescale differences. In contrast to thermalized ground-state reactions, there is no apparent relationship between the rate of transition and the density of vibrational states as approximately given by the molecular size (Figure 1).

[\*] T. S. Kuhlman, Prof. K. B. Møller  
Department of Chemistry, Technical University of Denmark  
Kemitorvet 207, 2800 Kgs. Lyngby (Denmark)  
E-mail: klaus.moller@kemi.dtu.dk

Prof. M. Pittelkow, Prof. T. I. Sølling  
Department of Chemistry, University of Copenhagen  
Universitetsparken 5, 2100 København Ø (Denmark)  
E-mail: theis@kiku.dk

[\*\*] T.I.S. acknowledges the Villum foundation and M.P. acknowledges the Danish Council for Independent Research/Natural Sciences and the Lundbeck Foundation for financial support. The Danish Center for Scientific Computing (DCSC) is acknowledged for computational resources.

Supporting information for this article is available on the WWW under <http://dx.doi.org/10.1002/ange.201208197>.

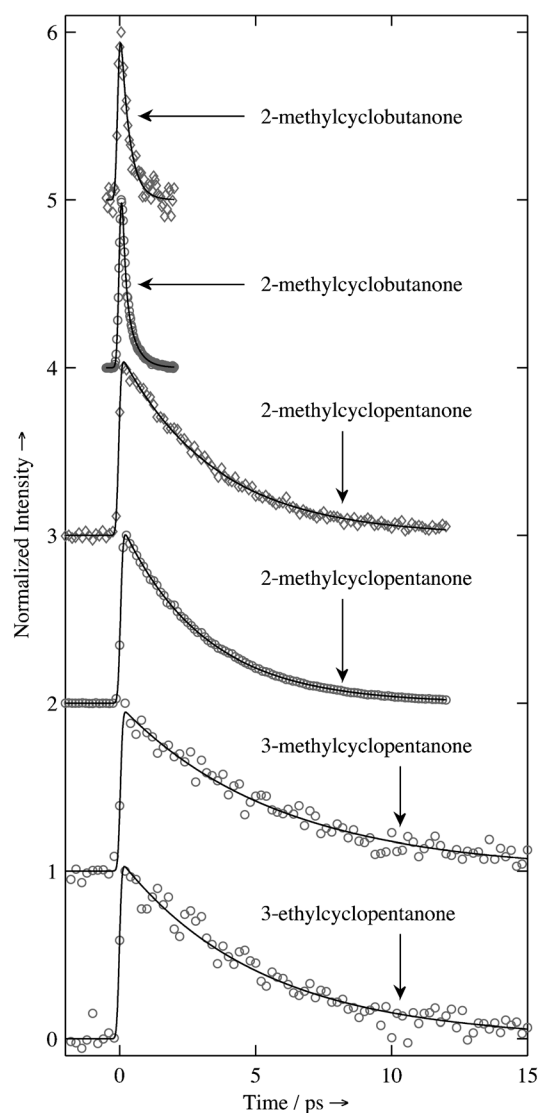


**Figure 2.** Temporal evolution of the normalized parent ion current for the four substituted cycloketones (○), and the normalized (*n*,3s) photoelectron current (◇). The different transients are displaced vertically by 1.0. The respective fitted kinetic models are indicated by the lines.

TRPES provides more information than the timescale for electronic population transfer. Figure 3 depicts the transient of the spectrally integrated (*n*,3s) photoelectron peak of 2-MeCP, where the integration has been performed over the lower and upper energy halves of the peak separately (see the Supporting Information). Such an integration scheme reveals a spectrally oscillating feature of the peak with a period of  $0.42 \pm 0.01$  ps (Table 2)—an unequivocal sign of nuclear motion affecting the electronic structure. The period corresponds to a frequency of about  $80\text{ cm}^{-1}$ , thereby revealing exactly which vibrational mode is dominant in mediating the coupling between the two electronic states. In the ground state, this low-frequency ring-puckering mode primarily involves the C-CO-C moiety of the molecule with the carbonyl group bending out of the molecular plane (see the Supporting Information). A similar oscillatory feature of the

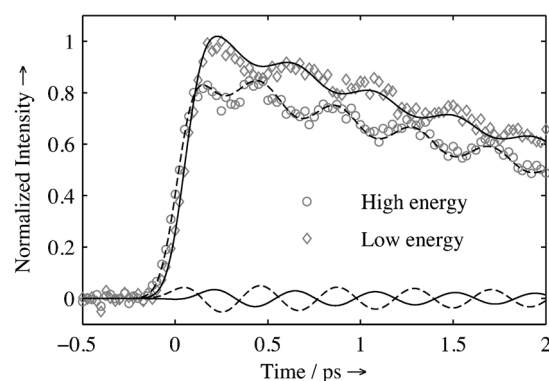


**Figure 3.** Temporal evolution of the low- and high-energy part of the (*n*,3s) photoelectron peak for 2-methylcyclopentanone along with the respective fitted kinetic models indicated by the lines. The oscillating component of each kinetic model is also given showing a clear phase relationship.

**Table 2:** Timescales for the decay of the (*n*,3s) photoelectron peak for two substituted cycloketones along with their unsubstituted species. Also given in two cases is the period, *T*, of the oscillation in energy of the peak.

Molecule	$\tau_1$ [ps]	$\tau_2$ [ps]	<i>T</i> [ps]
cyclobutanone <sup>[a]</sup>	$0.31 \pm 0.06$	$0.74 \pm 0.02$	$0.95 \pm 0.05$
2-methylcyclobutanone		$0.32 \pm 0.02$	
cyclopentanone <sup>[a]</sup>		$5.37 \pm 0.11$	
2-methylcyclopentanone		$3.47 \pm 0.03$	$0.42 \pm 0.01$ <sup>[b]</sup>

[a] From Ref. [6]. [b] Average period of the oscillation from the fit to the low- and high-energy parts of the (*n*,3s) photoelectron peak.

(*n*,3s) photoelectron peak was previously observed for CB. However, for CB the period of oscillation of  $0.95 \pm 0.05$  ps corresponds to a much lower vibrational frequency of about  $35\text{ cm}^{-1}$ .<sup>[6]</sup> This large difference in frequency is an important factor in explaining the observed different timescales, however, it is not fully sufficient on its own. As we will show below, at least three factors have to be taken into account: the frequency of the specific vibrational mode involved, the difference in energy of the excited state between the Franck–Condon and equilibrium geometries, that is, the difference of vertical and adiabatic excitation energies, and the total density of vibrational states of the molecule.

The distinct ability of the different molecules to more or less efficiently dispose of the electronic energy upon photoexcitation as given by the timescale of the (*n*,3s)→(*n*,π\*) transition can be rationalized by considering the model depicted in Figure 4. Once excited to the (*n*,3s) state the molecule will vibrate in some modes and the TRPES data show that only one (or a few) of these plays an important role in the route to the lower electronic state. We will restrict ourselves to a one-dimensional representation. In one dimension, the position of the crossing point with the lower electronic surface (or possibly avoided crossing) is given by two factors: the frequency of the vibrational mode in question and the energy difference between the Franck–Condon and equilibrium geometries of the excited state. A low frequency, that is, a small curvature, and a large energy difference will

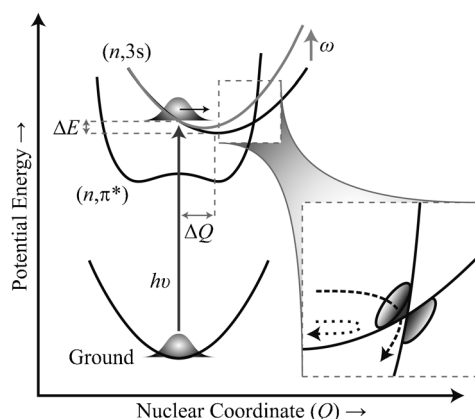


**Figure 4.** The vibrational frequency  $\omega$  and the energy difference  $\Delta E$  determine the intersection point between the two excited states. These two parameters thereby determine how close the molecule can get to the intersection point and, thus, the rate of nonadiabatic transition. The enlarged region shows two possible pathways: one adiabatic indicated by the dotted arrow and one nonadiabatic transition through a conical intersection indicated by the dashed arrow.

allow the molecule to access a larger configurational space, whereby it can more easily access the region near the very important conical intersection crossing point<sup>[8]</sup> leading to a faster nonadiabatic transition. Such a transition is illustrated by the dashed arrow in Figure 4 as opposed to the adiabatic dynamics indicated by the dotted arrow.

The cause of the intergroup timescale differences is primarily rooted in the energy difference factor, which is apparent by comparison of the unsubstituted cycloketones. The smaller, strained CB is able to relieve ring-strain in the  $(n,3s)$  state through vibration in the ring-puckering mode, whereas the five-membered ring of CP is less prone to such motion. As calculated using equation of motion coupled-cluster singles and doubles (EOM-CCSD), the energy difference in the  $(n,3s)$  state between the Franck–Condon and equilibrium geometries is 0.32 eV for CB, whereas it is only 0.14 eV for CP (see the Supporting Information). The more vibrationally congested  $(n,3s)$  absorption spectrum for CB compared to CP further corroborates this difference.<sup>[9]</sup> The even slower transition in cyclohexanone can be understood in terms of the inverse relationship between ring size and intensity of vibrational bands and, thus, release of angle strain in the C-CO-C moiety.<sup>[10]</sup> The frequency factor, as caused by different curvatures of the potential-energy surface illustrated by the two examples in Figure 4, also contributes to the intergroup timescale differences. The effect is clearly demonstrated by the observed anti-correlation between the vibrational frequency and the rate of transition for CB and 2-MeCP.

The intragroup timescale differences can largely be understood in terms of the frequency factor and how this is affected by substitution. Alkyl substitution in the 2-position leads to a significantly increased rate of transition, whereas this is not the case for substitution in the 3-position as observed when comparing 2-MeCP and 3-MeCP. The central vibrational mode primarily involves motion in the C-CO-C moiety, thus substitution in the 2-position should have a larger

effect on the rate of transition compared to the 3-position as it is indeed the case. This observation in turn confirms the conclusion on the non-ergodicity of the process hinted at in our previous work.<sup>[6]</sup> That is, the dynamics are truly localized in real space. The intergroup timescale differences also reflect this locality, as the apparent nonlocal change of the ring size actually has a very large local effect by significantly affecting the angle of the central C-CO-C moiety.

Although it has been stressed that the dynamics leading to disposal of the electronic energy is truly localized, an increase in the total density of vibrational states on the lower surface does slightly speed up the process. This effect is a consequence of additional vibrational degrees of freedom acting as acceptor modes in the lower electronic state. Comparison between the rates of transition for molecules of different ring sizes does not immediately reveal this aspect as the two other effects discussed play a much larger role. This aspect is, however, revealed by a comparison between the rates of transition for 3-MeCP and 3-EtCP. The addition of an extra  $\text{CH}_2$  group increases the density of vibrational states by a factor of about 100 at an energy of 2 eV—approximately the energy difference between the  $(n,3s)$  and  $(n,\pi^*)$  states (see the Supporting Information). However, this factor of 100 only leads to a small decrease in the timescale for transitions from  $5.79 \pm 0.16$  ps to  $5.16 \pm 0.17$  ps—very different from the behavior expected by application of theory in the statistical limit.<sup>[11–14]</sup>

Herein, we have revealed some salient features of the complex process of internal conversion. Most conclusions derived from the observation that the dynamics leading to a transition from one electronic state to another, and thereby to the transformation of electronic energy into vibrational energy, is inherently localized—only one or a few vibrational modes play a significant role. Merely by small structural variations, the vibrational frequency and the energy available in the excited state can be affected thereby tuning the rate of internal conversion over a range of more than an order of magnitude. A lower frequency and a larger available energy result in a faster process as the molecule can reach a configurational space in closer proximity of the crossing point between the excited states. The total density of vibrational states plays a smaller, secondary role as an increase in this only leads to a very slight increase in the overall rate. In contrast to the standard energy gap laws that neglect the nuclear dependence on the electronic coupling,<sup>[12,13]</sup> our results clearly show the effect of coherent nuclear motion on these matrix elements.

Received: October 11, 2012

Revised: December 31, 2012

Published online: January 16, 2013

**Keywords:** gas-phase reactions · kinetics · photophysics · time-resolved spectroscopy

[1] H. Fidler, M. Rini, E. T. J. Nibbering, *J. Am. Chem. Soc.* **2004**, *126*, 3789–3794.

- [2] N. J. Turro, V. Ramamurthy, J. C. Scaiano, *Modern Molecular Photochemistry of Organic Molecules*, University Science Books, Sausalito, CA, **2010**.
- [3] E. W.-G. Diau, J. L. Herek, Z. H. Kim, A. H. Zewail, *Science* **1998**, 279, 847–851.
- [4] O. Schalk, A. E. Boguslavskiy, A. Stolow, *J. Phys. Chem. A* **2010**, 114, 4058–4064.
- [5] T. S. Kuhlman, W. J. Glover, T. Mori, K. B. Møller, T. J. Martínez, *Faraday Discuss.* **2012**, 157, 193–212.
- [6] T. S. Kuhlman, T. I. Sølling, K. B. Møller, *ChemPhysChem* **2012**, 13, 820–827.
- [7] T. S. Kuhlman, S. P. A. Sauer, T. I. Sølling, K. B. Møller, *J. Chem. Phys.* **2012**, 137, 22A522.
- [8] T. J. Martínez, *Nature* **2010**, 467, 412–413.
- [9] L. O'Toole, P. Brint, C. Kosmidis, G. Boulakis, P. Tsekeris, *J. Chem. Soc. Faraday Trans.* **1991**, 87, 3343–3351.
- [10] T. J. Cornish, T. Baer, *J. Am. Chem. Soc.* **1987**, 109, 6915–6920.
- [11] R. A. Marcus, *J. Chem. Phys.* **1952**, 20, 359–364.
- [12] M. Bixon, J. Jortner, *J. Chem. Phys.* **1968**, 48, 715–726.
- [13] R. Englman, J. Jortner, *Mol. Phys.* **1970**, 18, 145–164.
- [14] K. B. Møller, A. H. Zewail in *Essays in Contemporary Chemistry: From Molecular Structure towards Biology* (Eds.: G. Quinkert, M. V. Kisakürek), Verlag Helvetica Chimica Acta, Zürich, and Wiley-VCH, Weinheim, **2001**, chap. 5, pp. 157–188.